

Direct noise computation of a Mach 3.30 jet

N. de Cacqueray, C. Bogey, C. Bailly & D. Juvé

Centre Acoustique, LMFA, UMR 5509

Ecole Centrale de Lyon

<http://acoustique.ec-lyon.fr>

- Introduction
- Present study
 - simulation parameters
 - numerical methods
- Flow field
 - mean flow field properties
 - turbulent flow features along the shear layer
- Acoustic field
 - acoustic near field
 - acoustic far field
- Concluding remarks

Context (1)

- Vibrations at lift off on space launchers induced by acoustic waves
 - propulsive jet noise
 - blast wave

- Propulsive jets properties

- supersonic flow: $M_e > 2$
- not perfectly expanded: $p_e \neq p_\infty$
- very high values of stagnation quantities:
 $T_r > 1000 \text{ K}$ and $P_r > 25 \text{ bar}$



- very few experimental facilities exist for these conditions
(in France: MARTEL facility in Poitiers)
- numerical simulations difficult but now feasible

Context (2)

• Radiation mechanisms in supersonic jets

- **turbulent mixing** noise

Laufer *et al.*, *AIAA J.*, 1976, Panda & Seasholtz, *JFM*, 2002

- **broadband shock-associated noise**

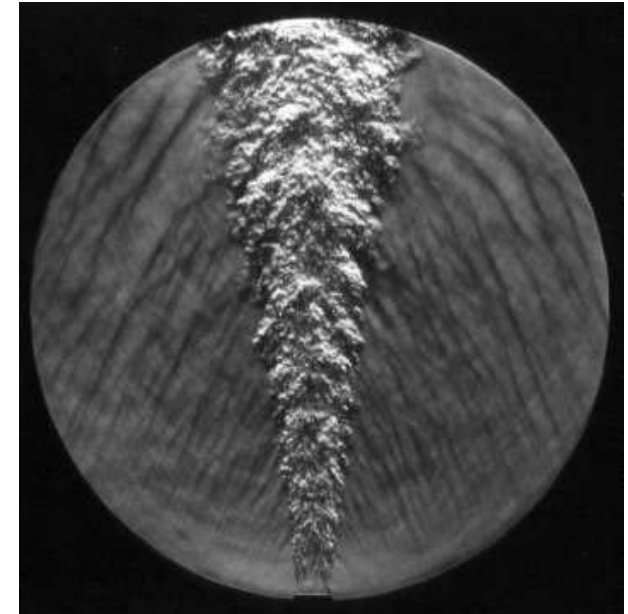
Tam & Tanna, *JSV*, 1982, Seiner & Yu, *AIAA J.*, 1984

- **screech** noise

Powell *et al.*, *JASA*, 1992, Berland *et al.*, *PoF*, 2007

- **Mach wave** radiation

McLaughlin *et al.*, *JFM*, 1975, Tam *et al.*, *AIAA J.*, 1992



He jet at $M_e = 2$

Clemens & Paul, *PoF*, 1993

• Radiation mechanisms in propulsive jets ($M_e > 2$)

- **Mach waves are expected to be dominant**

Tam & Hu, *JFM*, 1989, Tam *et al.*, *AIAA J.*, 1992

- contribution of other noise radiation mechanisms to be quantified

Outline

- Introduction
- Present study
 - simulation parameters (*for details see de Cacqueray & al., AIAA 2010-3732*)
 - numerical methods
- Flow field
 - mean flow field properties
 - turbulent flow features along the shear layer
- Acoustic field
 - acoustic near field
 - acoustic far field
- Concluding remarks

Simulation parameters

• Jet exit conditions

- exit quantities : $M_e = 3.3$, $P_e = 0.5$ bar and $T_e = 360$ K ($M_a = 3.47$)
(stagnation temperature $T_r = 1144$ K)
- boundary layer thickness at the nozzle exit : $\delta/r_e = 0.05$
- maximum velocity fluctuations at the nozzle exit : $u'_{rms}/u_e = 0.3\%$

	Mach M_e	Pressure P_e	Temperature T_e	Reynolds Re
Present computation	3.30	0.50×10^5 Pa	360 K	0.94×10^5
Experiment*	3.27	0.51×10^5 Pa	359 K	17.5×10^5

* Varnier & Gély, RT 112/3643, 1998

• LES numerical parameters

- **cylindrical mesh** : $n_r \times n_z \times n_\theta = 256 \times 840 \times 128 = 28 \times 10^6$ points
- CPU time : 500 hours on a NEC SX-8 (120,000 iterations)

• Far-field wave extrapolation

- LES data are propagated to $r = 80r_e$ from the nozzle exit
- full **non linear Euler equations** are solved on a grid containing 210×10^6 points

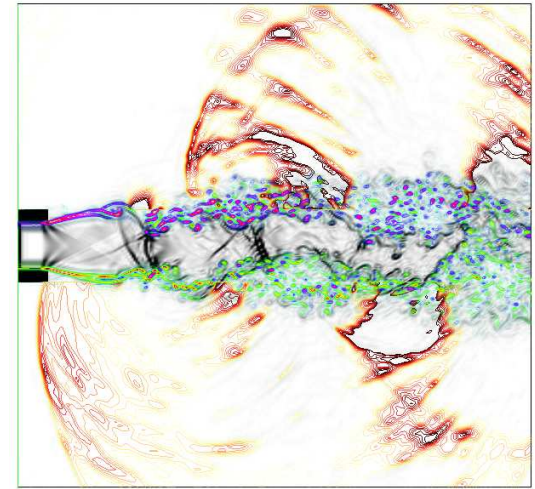
• Cut-off Strouhal number and simulation time

- $St_c \approx 1.4$; $T = 540T_c = 540D_e/U_e$

Numerical approach

• Direct Noise Computation

- aerodynamic and acoustic fields are **solved simultaneously** using Navier-Stokes equations
- successful applications to **subsonic and supersonic jets**



Berland, Bogey & Bailly
Phys. of Fluids, 2007

• Large-Eddy Simulation based on Relaxation-Filtering

Bogey & Bailly, *J. Fluid Mech.*, 2009, 626

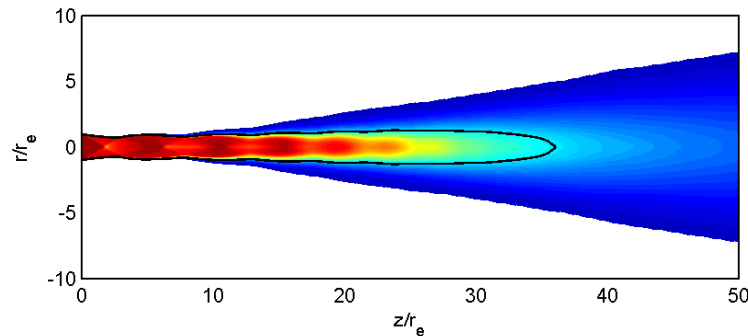
• In-house finite-difference solver

- **low-dissipation** and **low-dispersion** schemes
Bogey & Bailly, *J. Comput. Phys.*, 2004, 194(1)
Berland, Marsden, Bogey & Bailly, *J. Comput. Phys.*, 2007, 224
- **non-reflective boundary** conditions and sponge zone
Bogey & Bailly, *Acta Acustica*, 2002, 88(4)
- **adaptative** and **conservative shock-capturing** method
Bogey, de Cacqueray & Bailly, *J. Comput. Phys.*, 2009, 228(5)

- Introduction
- Present study
 - simulation parameters
 - numerical methods
- Flow field
 - mean flow field properties
 - turbulent flow features along the lip line
- Acoustic field
 - acoustic near field
 - acoustic far field
- Concluding remarks

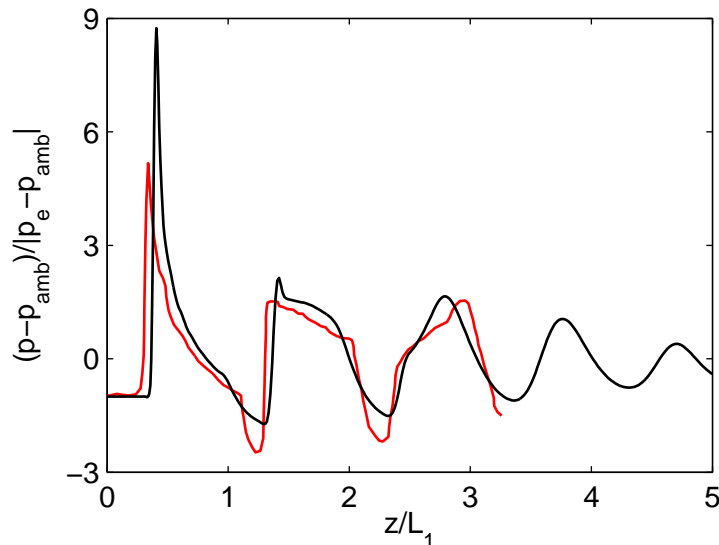
Mean flow field properties

• Mean axial velocity



- sonic core : $L_s = 36r_e$
- potential core : $L_c = 20r_e$
- MARTEL exp. : $L_s = 50r_e$ and $L_c = 24r_e$

• Centerline mean static pressure



	M_e	M_j	L_1	$ p_e - p_{amb} $
Present LES	3.3	2.83	$4.6r_e$	$0.5 \times 10^5 \text{ Pa}$
N & S*	2	1.82	$3r_e$	$0.2 \times 10^5 \text{ Pa}$

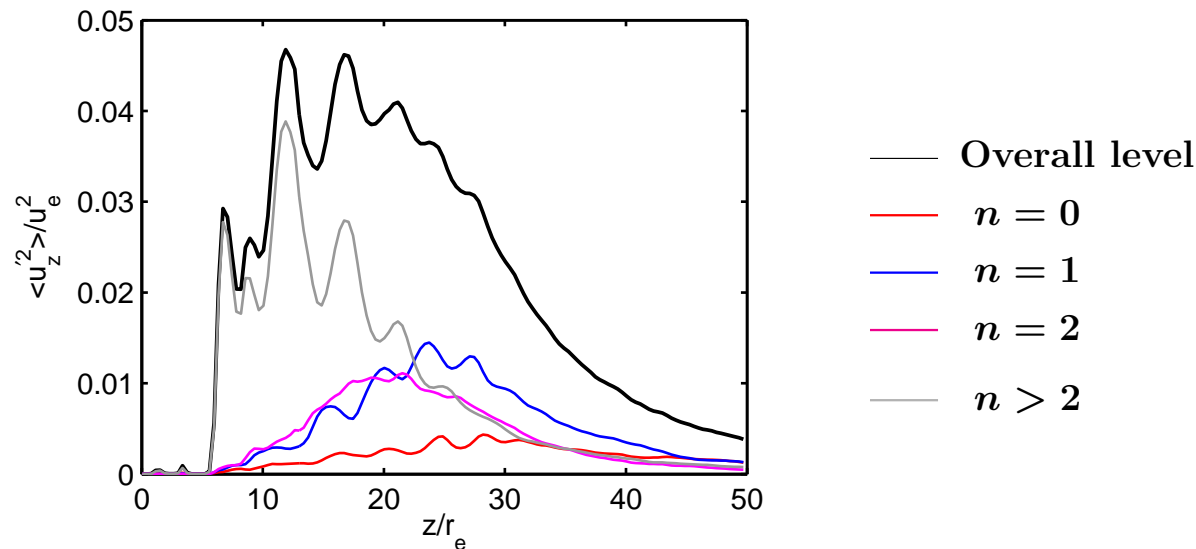
rum & Seiner, NASA TM 84521, 1982

vspace/3cm * No-

→ the shape of the first three shocks agrees reasonably well with experimental data (with proper scaling)

Turbulent flow (1)

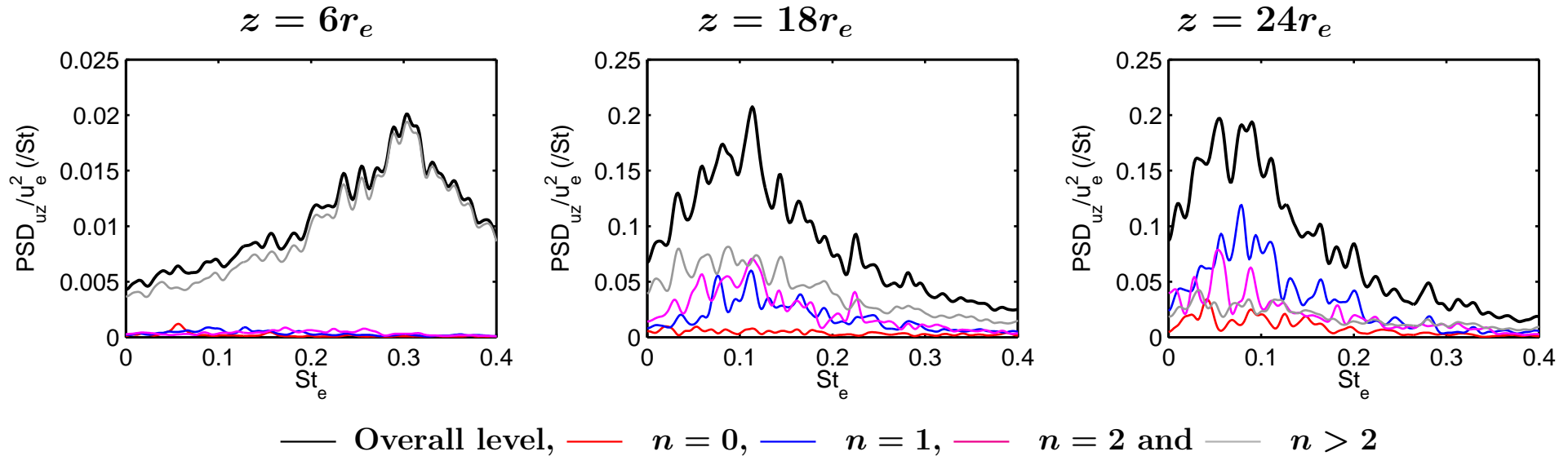
- Longitudinal turbulent fluctuations and azimuthal decomposition along $r = r_j$



- **before the end of the potential core:** ($z < 20r_e$)
 - azimuthal modes $n > 2$ dominate
 - contribution of modes $n = 0$, $n = 1$ and $n = 2$ increases with axial distance
 - mode $n = 0$ has a low contribution
- **after the end of the potential core:** ($z > 20r_e$)
 - mode $n = 1$ dominates

Turbulent flow (2)

- Frequency analysis of modal components of u'_z at $z = 6, 18$ and 24 , for $r = r_j$

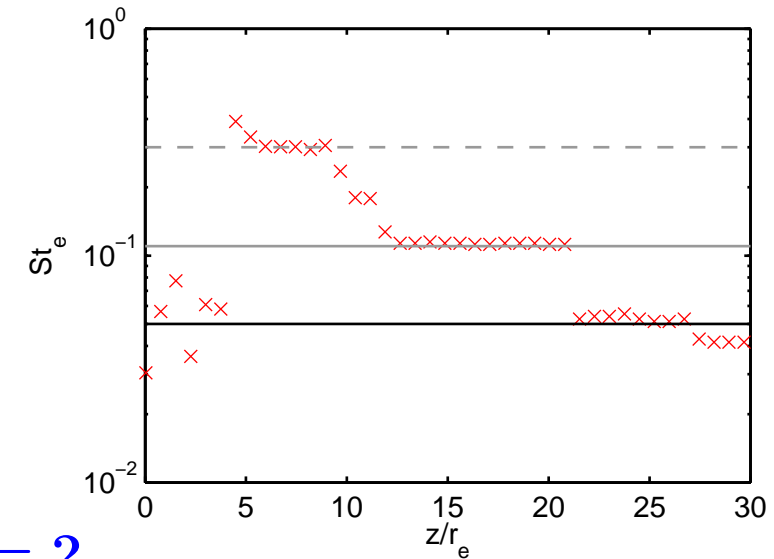


- $z = 6r_e$: connections between the peak at $\text{St}_e = 0.3$ and higher order modes
- $z = 18r_e$: peaks at $\text{St}_e = 0.08$, 0.11 and 0.22
- $z = 24r_e$:
 - peaks at $\text{St}_e = 0.05$, 0.08 , 0.09 and 0.11
 - the peak at $\text{St}_e = 0.08$ seems connected to mode $n = 1$
 - mode $n = 0$ emerges with a maximum at $\text{St}_e = 0.04$

Turbulent flow (3)

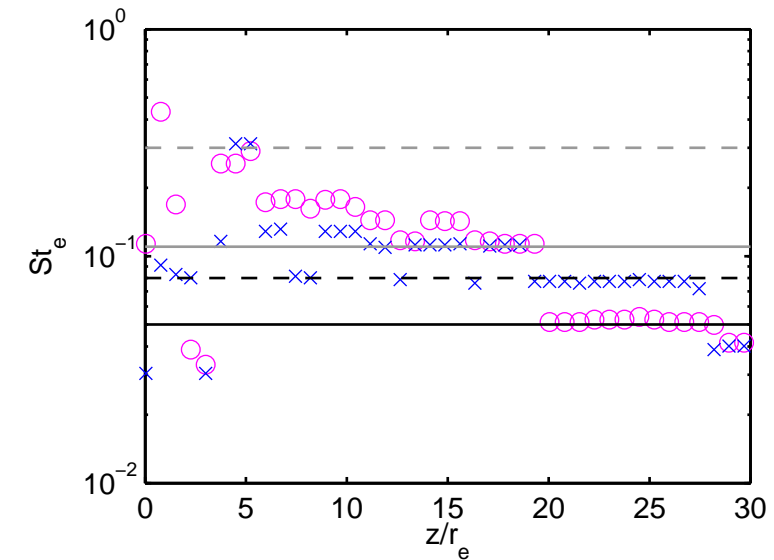
• Peak Strouhal numbers of u'_z at $r = r_j$

- before the end of the potential core ($z < 20r_e$)
 - peaks at $St_e = 0.3$ and $St_e = 0.11$
 - **connected to a change of shock motion**
- after the end of the potential core ($z > 20r_e$)
 - peaks at $St_e = 0.05$



• Peak Strouhal numbers of modes $n = 1$ and $n = 2$

- before the end of the potential core ($z < 20r_e$)
 - peaks between $St_e = 0.1$ and $St_e = 0.17$
 - **peaks at $St_e = 0.08$ for $n = 1$**
 - are also noticed**
- after the end of the potential core ($z > 20r_e$)
 - peaks at $St_e = 0.05$ for mode $n = 2$
 - peaks at $St_e = 0.08$ for mode $n = 1$



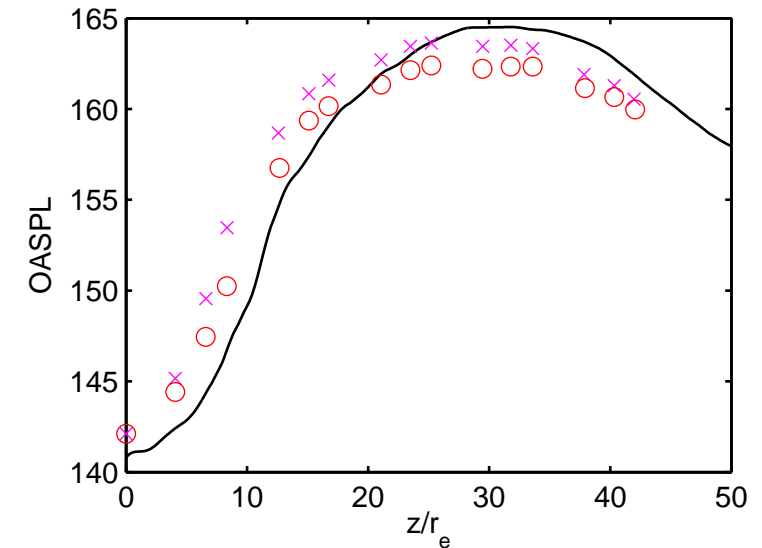
x n=1, o n=2

- Introduction
- Present study
 - simulation parameters
 - numerical methods
- Flow field
 - mean flow field properties
 - turbulent flow features along the shear layer
- Acoustic field
 - acoustic near field
 - into the acoustic far field
- Concluding remarks

Near field OASPL

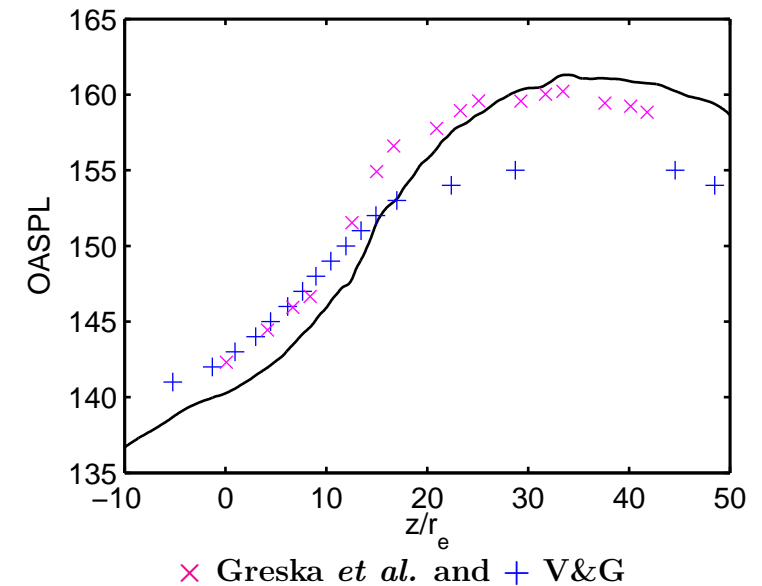
• Overall pressure levels at $r = 9.5r_e$

- measurements of Greska *et al.*:
present LES $M_e = 3.3$ $M_j = 2.83$ $M_a = 3.5$
Greska exp. $M_e = 2$ $M_j = 2$ $M_a = 3$
(* AIAA Paper 2008-3026)
- maximum of OASPL around $z = 30r_e$
- rapid growth between $z = 7r_e$ and $z = 20r_e$



• Overall pressure levels at $r = 16r_e$

- measurements of Greska *et al.* and V&G
AIAA Paper 2008-3026
Varnier & Gély, ONERA, RT 112/3643
- 5dB difference between V&G and Greska
(effect of Reynolds number, nozzle exit conditions or reservoir conditions?)



→ good agreement between computation and experiments

Acoustic near field at 9.5 radii (1)

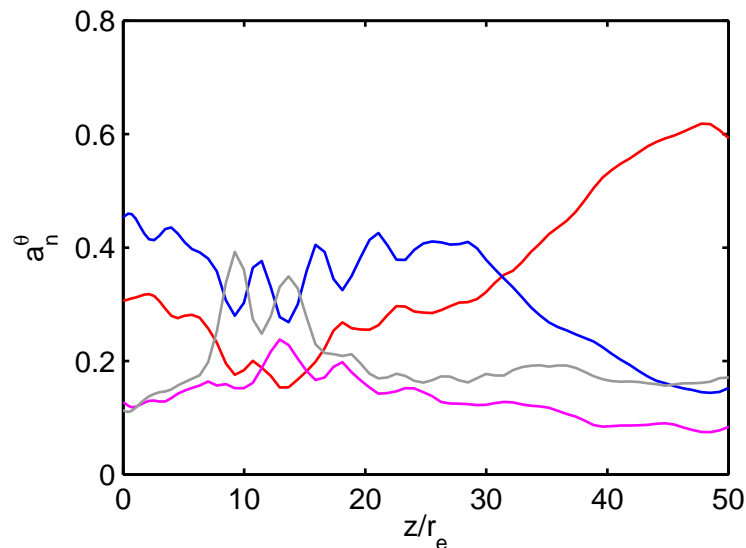
• Azimuthal decomposition

- azimuthal cross-correlation functions:

$$R^\theta(\delta\theta) = \frac{\langle p'(\theta)p'(\theta + \delta\theta) \rangle}{\langle p'^2(\theta) \rangle^{1/2} \langle p'^2(\theta + \delta\theta) \rangle^{1/2}}$$

- Fourier sum:

$$R^\theta(\delta\theta) = \sum_{n=0}^{\infty} a_n^\theta \cos(n\delta\theta)$$



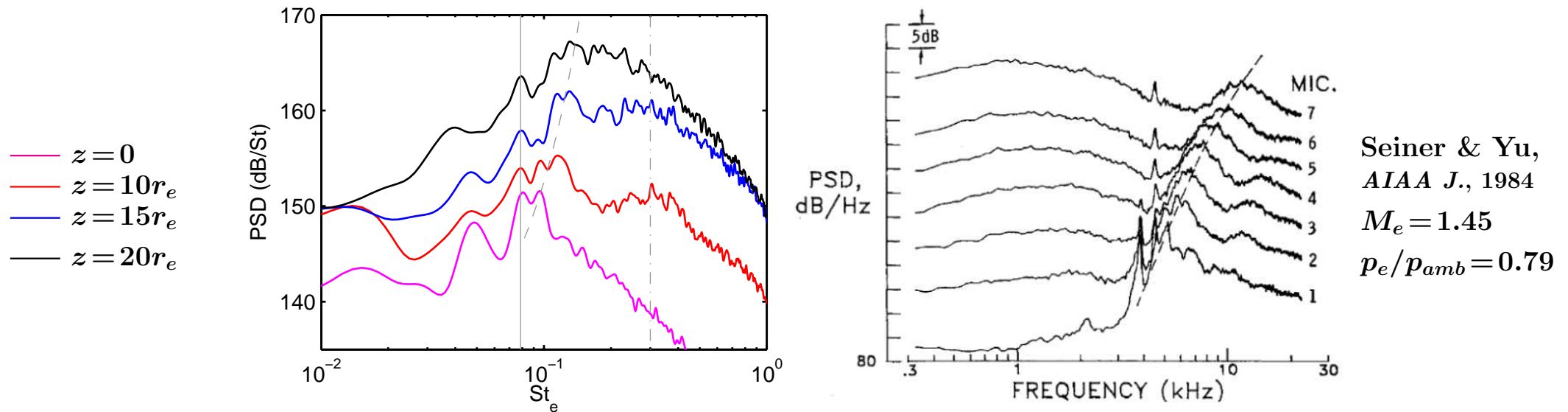
→ modes $n = 0$ and $n = 1$ are predominant

→ the acoustic field is less correlated between $z = 7r_e$ and $z = 16r_e$

— $n = 0$, — $n = 1$, — $n = 2$ and — $n > 2$

Acoustic near field at 9.5 radii (2)

- Acoustic spectra between $z = 0$ and $z = 20r_e$



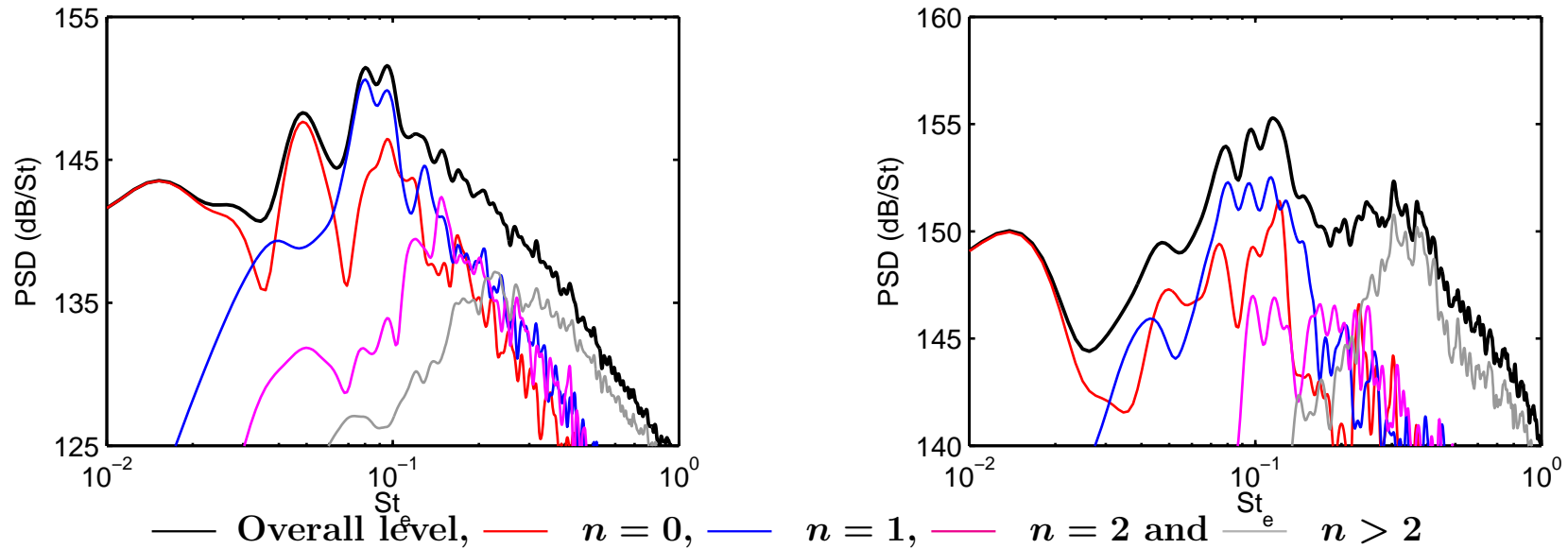
- upstream propagating shock-associated noise (Tam *et al.*, *JSV*, 1986)

$$St_{up} = \frac{2r_e u_c / u_e}{L_{shock}(1 + M_c)} = 0.079$$

- low-frequency component observed at $St_e = 0.05$
- 'high-frequency' broadband noise around $St_e = 0.3$
- broadband spectra at $z = 20r_e$
- a qualitative agreement is noticed with near-field measurements by Seiner & Yu for the moving peak

Acoustic near field at 9.5 radii (3)

- Azimuthal decomposition at $z = 0$ and $z = 10r_e$



- modes $n = 0$ and $n = 1$ dominate for low frequencies
 - peak at $St_e = 0.05$ associated with mode $n = 0$
 - peak at $St_e = 0.08$ associated with mode $n = 1$
- at $z = 10r_e$, the **broadband** noise centered at $St_e = 0.3$ is linked to **azimuthal modes higher than 2**

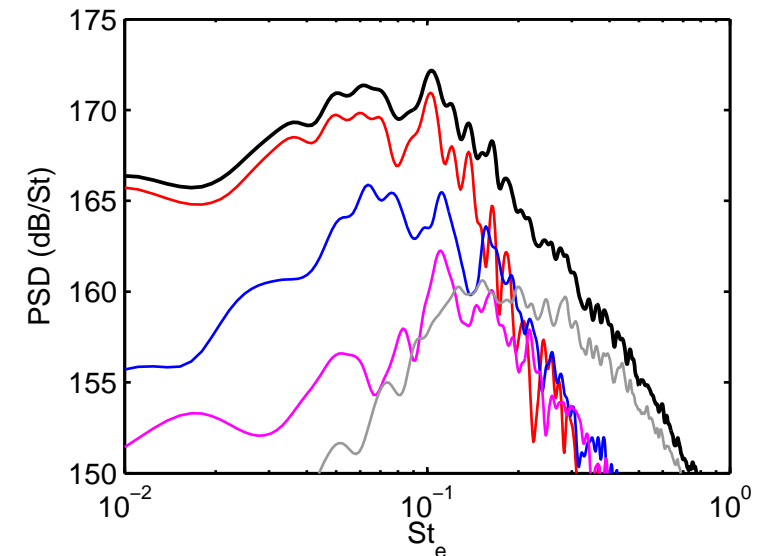
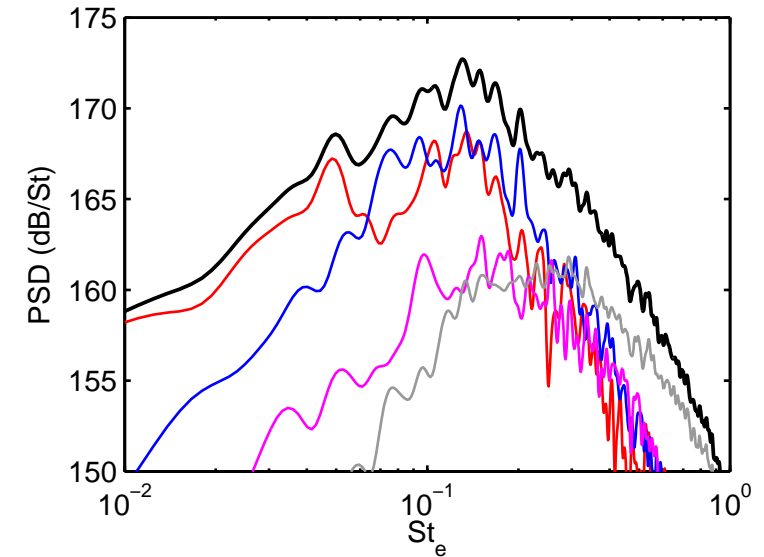
Acoustic near field at 9.5 radii (4)

• Azimuthal decomposition at $z = 30r_e$

- $z = 30r_e$ corresponds to the maximum of the OASPL
- modes $n = 0$ and $n = 1$ dominate
- the maximum at $St_e = 0.13$ is linked to mode $n = 1$
- a peak at $St_e = 0.05$ is linked to mode $n = 0$

• Azimuthal decomposition at $z = 40r_e$

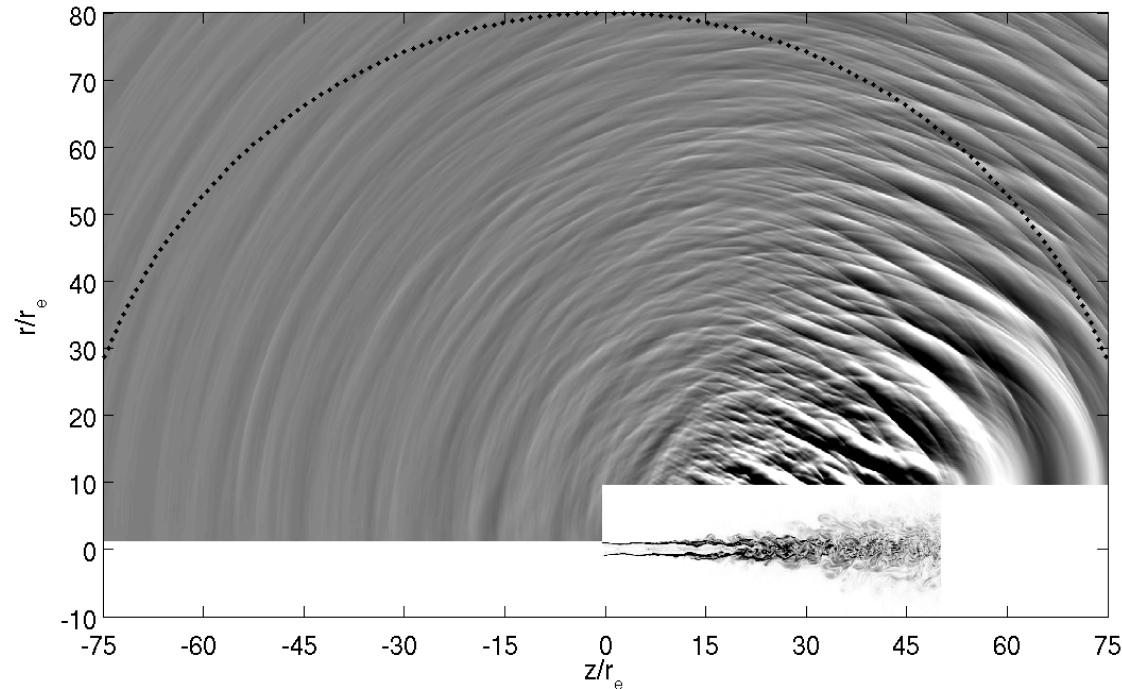
- mode $n = 0$ dominates
- two peaks at: $St_e \approx 0.055$ and $St_e = 0.1$ (axial velocity fluctuations after end of potential core: $St_e = 0.05$)



— Overall level, — $n = 0$, — $n = 1$, — $n = 2$ and — $n > 2$

Acoustic far field (1)

- Acoustic far field

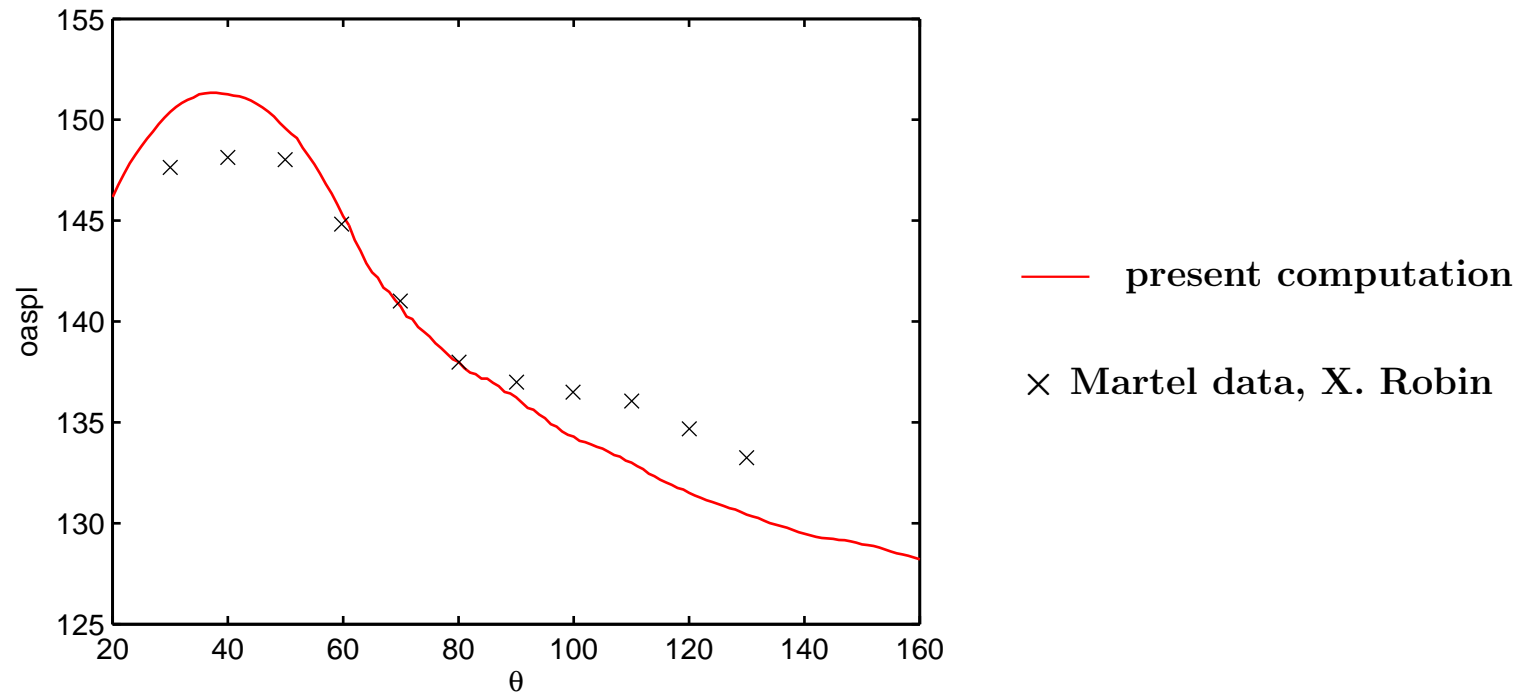


- acoustic waves are propagated to a distance of 80 radii, starting from a control surface located at $r = 9.5r_e$
- full (non linear) Euler equations are solved
- same numerical methods are used including the shock-capturing procedure

Mach wave radiation apparent for $\theta = 60^\circ$ (very close to expected value $\cos\theta = 1/M_c$)

Acoustic far field (2)

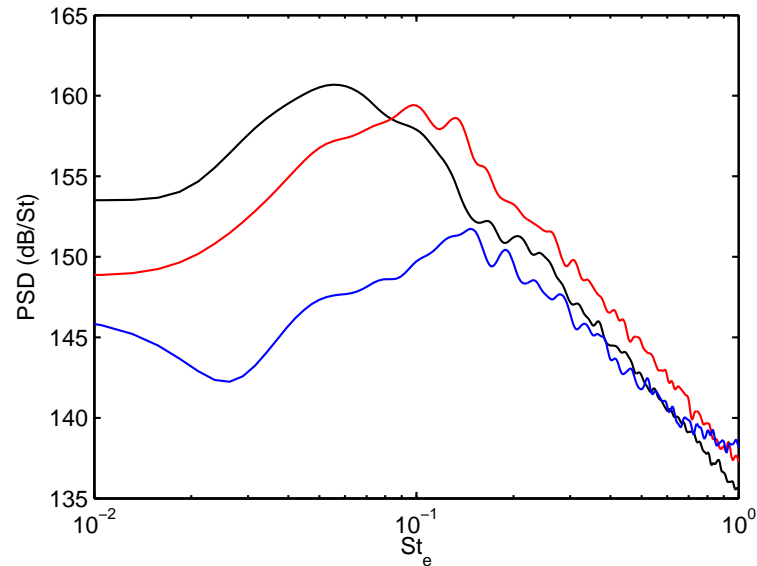
- Far field SPL compared to experimental data



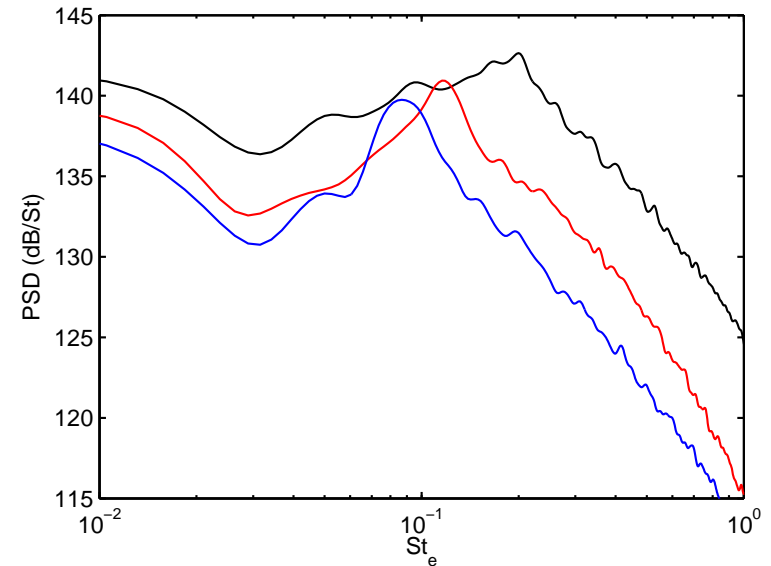
- good agreement with experimental data
- peak SPL 3-4 dB higher than measurements
- note that V&G (Martel) near field data already 5 dB lower than Greska (in downstream direction), and that operating conditions are not fully comparable

Acoustic spectra

• Acoustic spectra



— $\theta = 30^\circ$, — $\theta = 45^\circ$, — $\theta = 60^\circ$

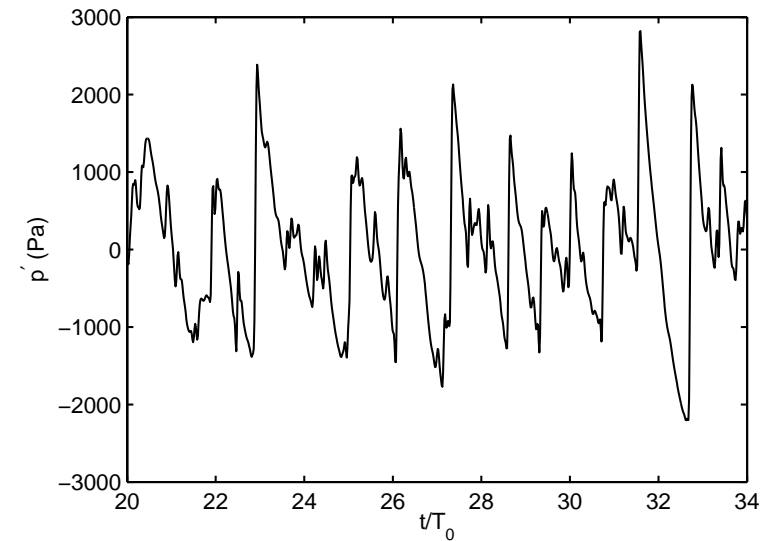
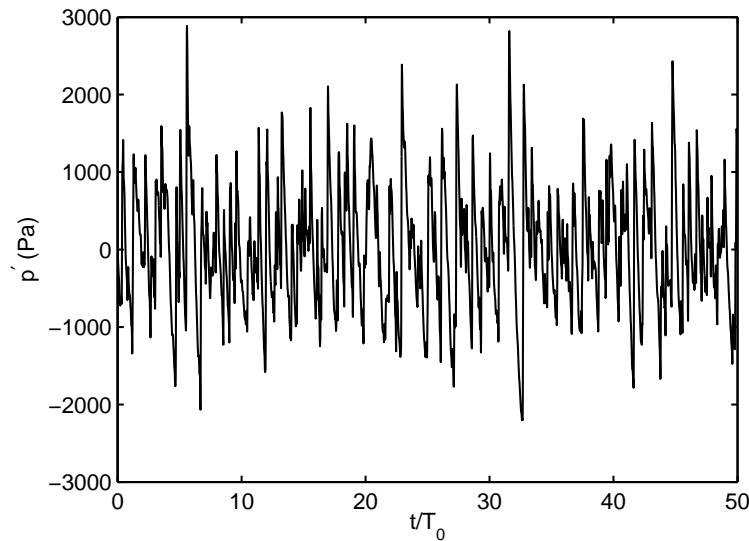


— $\theta = 90^\circ$, — $\theta = 120^\circ$, — $\theta = 150^\circ$

- evidence of shock associated noise in the rear arc
($St_e = .09$ & $.12$ for $\theta = 150^\circ$ & 120°)
- nothing special at Mach wave radiation angle
(slight reinforcement of high frequencies?)

Mach wave radiation

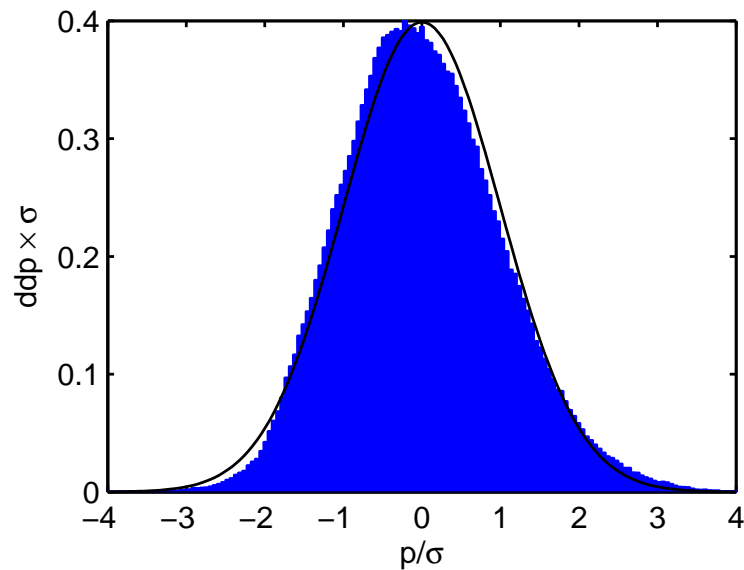
- Time evolution of acoustic pressure in Mach wave direction



- positive peaks generally larger than negative ones
- consequence: non-gaussian, skewed pdf
- indication of ”‘crackle’” component?

Mach wave radiation (2)

• Pdf of pressure signal



— Gaussian distribution

- **skewness factor** $k = \frac{\overline{p^3}}{(\overline{p^2})^{3/2}} \approx 0.4-0.45$
- value somewhat lower than in experiments (**crackle detectable for $k > .3$**); measured values up to $k = .8$.
- however **skewness tends to be lower for very high velocity jets as well as the contribution of Mach waves** to overall noise level in the peak radiation angle (see *Krothapalli & al., AIAA paper 2003-1200*)

Concluding remarks

- Aerodynamic field

- good qualitative agreement with the few experimental data available
- spectra of turbulent fluctuations exhibit low frequency peaks which may be associated to shock motion

- Acoustic field

- good agreement with experimental data for the near-field OASPL
- acoustic near field dominated by modes $n = 0$ and $n = 1$
- good agreement also with experimental data for far-field directivity.
Apparent overestimation of level in the direction of maximum radiation.
- shock-associated noise identified in upstream arc
- 'crackle' component present in the direction of Mach wave radiation

Concluding remarks

• Future work

- more detailed investigation of Mach wave component and relation to crackle
- azimuthal decomposition of far-field pressure and search for a link with turbulent fluctuations
- a second computation is currently running, with exit conditions comparable to recent Martel experiments (exit temperature $T_e = 750K$).
Detailed comparison of directivity and spectra to come!